JOURNAL OF MATERIALS SCIENCE **37** (2002) 3299–3306

Study of the interaction between graphite and Al-Si melts for the growth of crystalline silicon carbide

C. JACQUIER, D. CHAUSSENDE, G. FERRO*, J. C. VIALA, F. CAUWET, Y. MONTEIL
Laboratoire des Multimatériaux et Interfaces (UMR 56-15), Université Claude Bernard Lyon1, 43 Boulevard du, 11 novembre 1918, 69622 Villeurbanne, France
E-mail: ferro@univ-lyon1.fr

The chemical interaction between Al-Si melts of different compositions and graphite was investigated in order to clarify the mechanism of spontaneous growth of silicon carbide crystals from these melts. Calibrated graphite small rods were used as carbon source to facilitate comparison between experiments. For a temperature set to 1100°C, the reaction time and Si content of the melt were varied from 1 to 48 hours and 20 to 40 at.%, respectively. It has been found that in a first stage the liquid reacts at a relatively slow rate to form a microcrystalline SiC layer around the graphite rod. When this SiC layer has reached a certain thickness, a violent attack follows in some specific sites by rapid dissolution of the rod. Radial liquid channels progress from the surface of the rod up to its centre and then total conversion of graphite into SiC rapidly occurs. The local Si content of the melt, which controls the carbon solubility in the liquid, governs the overall mechanism. To form faceted β-SiC crystals, the growth mechanism should involve carbon dissolution in one place and supersaturation in another place in relation with local changes of the Si content in the melt.

1. Introduction

It is many decades since Liquid Phase Epitaxy (LPE) has been tentatively studied as an alternative for growing low cost SiC layers at a fast rate. Recently, it has proven to be the only technique which can "heal" the macro-defects of the commercially available substrates [1, 2]. However, LPE is difficult to operate because of the elevated temperatures (>1600°C) required for fast growth rate and the high reactivity and vapour pressure of silicon at these temperatures. The use of Si-based melts with a low melting temperature for growing SiC crystals by LPE is attractive to simplify the technique and reduce the fabrication costs. In this regard, aluminium is a good candidate for alloying with Si since an alloy with a melting point as low as 577°C can be obtained. Furthermore, the solubility of carbon in liquid aluminium is higher than in liquid silicon [3] so that faster growth rates can be expected. The feasibility of SiC growth by low temperature LPE has already been demonstrated in Al-Si based liquids to which Ga or Sn were added [4]. Growth rates of 0.1 to 1 μm/h were reported at temperatures ranging from 1100 to 1200°C. However, very little is known about the phase relations and equilibria in the quaternary systems Al-Si-Ga-C and Al-Si-Sn-C. The same is true for the adjacent ternaries [5–7], except the Al-Si-C system for which detailed data are available [3, 8]. According to the Al-Si-C ternary phase diagram, two solid carbides can form at temperatures lower than 1400°C: SiC and Al_4C_3. This diagram also shows that silicon rich alloys are needed to avoid formation of Al_4C_3.

In order to control the growth processes involved in the LPE of SiC in Al-Si melts, it is of interest to clarify the mechanisms of carbon dissolution in the source zone and of SiC nucleation in the deposition zone. The latter point has been studied in a previous work [9] by observing the change in size of SiC crystals spontaneously grown under isothermal conditions as a function of the Si content and temperature of the melt. It has been shown that the biggest SiC crystals, always of the cubic structure (β-SiC), were grown at 1100°C from an Al-Si melt with 30 at.% Si (Fig. 1). The reaction time was set to 48 hours and the carbon source was graphite powder. Under these optimum conditions, we demonstrated the possibility of epitaxial growth on a crystalline β-SiC seed as shown in Fig. 2.

In this study, we will focus on the processes involved in the source zone of LPE experiments, i.e., the mechanism and kinetics of the interaction between carbon and the Al-Si melts. The carbon source has been changed from graphite powder to small rods calibrated in diameter in order to allow a more precise and reproducible

*Author to whom all correspondence should be addressed.

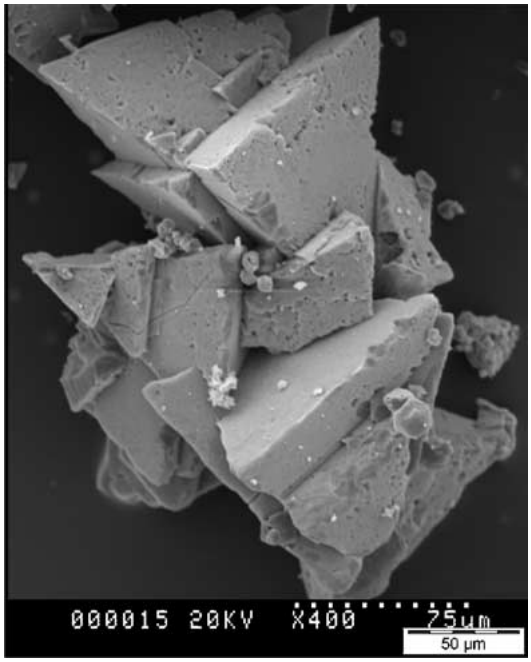

Figure 1 SEM microphotograph of β-SiC crystals spontaneously grown at 1100°C with an Al-Si melt of 30 at.% Si.

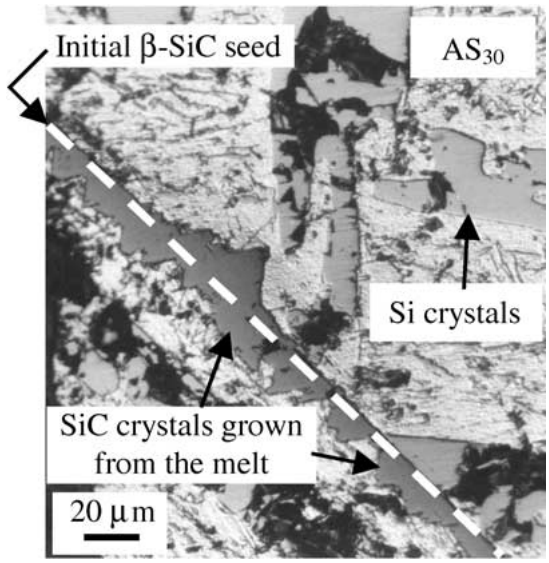

Figure 2 Growth of β-SiC crystals in epitaxial relationship with a 3 μm thick β-SiC seed achieved by CVD on silicon substrate. The Al-Si melt has dissolved the Si substrate and the self-standing SiC layer remained in the liquid.

characterisation of the graphite-melt reaction zone and facilitate therefore the elucidation of the mechanism of C dissolution in the melt.

2. Experimental set up

The Al, Si sources were respectively 99.5% Al powder and electronic grade (6N) Si powder. For the C source, we used 1.5 mm diameter Ellor +20 graphite rods from Carbone Lorraine with the following characteristics: density of 1.8, open porosity of 8–10%, mean grain size of 20 μm and ash residue lower than 0.3% in weight. First, the Al and Si powders were carefully mixed to give an homogeneous powder of the desired Si content. The graphite rod was then introduced in the mixed powder and cold-pressed with it under 240 MPa. Care was taken not to brake the rod during this procedure. The samples thus prepared were heated under a static argon pressure of 1 atm to limit Al loss by evaporation. The temperature was fixed at 1100°C, value at which the biggest SiC crystals were previously obtained [9]. The reaction time and Si content were varied from 1 to 48 hours and from 20 to 40 at.% respectively. As a rule, we will call AS_x a melt having a Si content of X at.%. After heat-treatment, the samples were observed in cross section by optical microscopy and analysed by micro-Raman spectroscopy. Two cross sections corresponding to different parts of the rod were systematically examined for each sample in order to check the uniformity of the interaction. When not specified, the two cross sections gave the same results. Formation of the Al_4C_3 phase has been identified either by micro-Raman spectroscopy or by simply observing the sample after several days of exposure to ambient moisture: on such an exposure, Al_4C_3 is the only compound in the Al-Si-C system that changes in aspect (colour change and volume expansion) by hydrolysing.

3. Results

We will first focus on the effect of reaction time for samples with a melt composition of 30 at.% Si (AS_{30}) as this is the composition for which the biggest β-SiC crystals were grown in our earlier study. The effect of varying the Si content will be presented afterward.

3.1. AS_{30} experiments

For short reaction times (a few hours), the reaction zone around the graphite rod is not uniform. Some parts of the rod are free of reaction zone. Where carbon has reacted, a 10 μm thick SiC layer is observed. For an experiment duration of 14 hours, the rod is almost completely covered with a thicker SiC layer: 30 μm instead of 10 μm (Fig. 3a). These observations suggest a progressive wetting of the graphite surface by the AS_{30} melt. It has been shown by Landry *et al*. that the wetting of various types of carbon by pure liquid Al or Al-Si alloys is time dependent [10]. The initial contact angle is as high as 160° and drops down to about 50° after more than 1h at 923°C. Higher temperatures lead to a faster decrease of the contact angle but the initial contact angle is always the same. In other words, the wetting of Al-Si alloys on graphite is not instantaneous and may be delayed even at high temperature.

In order to minimise the effect of delayed wetting on the extent and nature of the reaction zone, attention will mainly be paid to long reaction times, i.e., equal to or higher than 14 hours. Note also in Fig. 3a the presence, inside the Al-Si melt, of elongated silicon crystals that have grown upon cooling.

In Fig. 3b, we can see the scattered microstructure of the reaction zone in a place of the graphite surface where a little dip has begun to form. The first layer composed of SiC microcrystals tends to break up into fragments surrounded by liquid. A little away from the

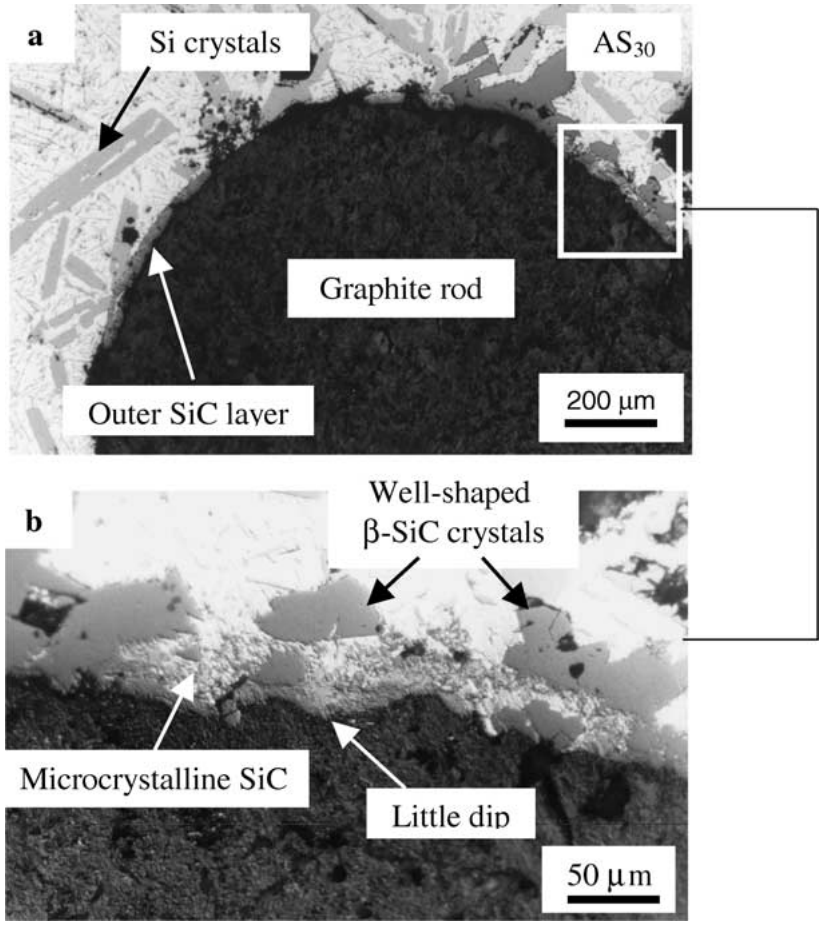

Figure 3 (a) Optical microphotograph showing a typical cross section of a graphite rod treated at 1100°C for 14 hours with a AS_{30} melt. The light grey elongated phase far from the rod consists of silicon crystals grown upon cooling of the sample. Only the outer part of the rod has reacted to form SiC; (b) Close up of a reaction zone showing the scattered microstructure of the SiC layer in direct contact with the rod. Note the small dip starting to form at the rod surface.

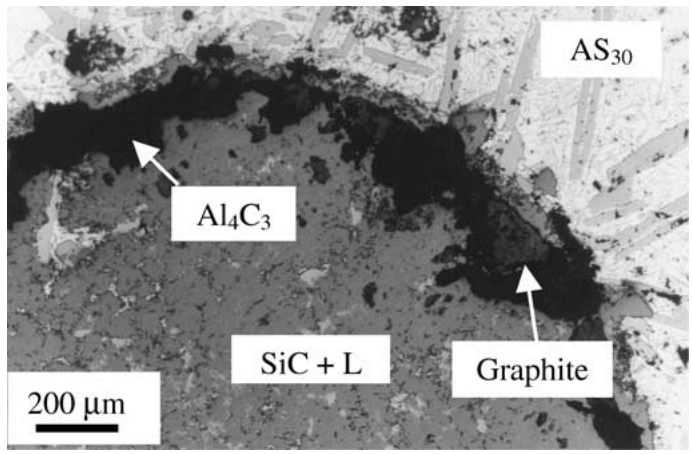

Figure 4 Optical microphotograph showing the cross section of a sample treated at 1100°C for 28 hours with a AS_{30} melt.

rod edge, faceted crystals of β-SiC (as characterised by Raman spectroscopy) are found. For that sample, the main body of the graphite rod has not reacted and no Al_4C_3 is detectable.

After 28 hours, the sample shows two different degrees of interaction according to the cross sections examined. In one section, the carbon rod looks like in Fig. 3: only its outer part has reacted to give a 40 μm thick microcrystalline SiC layer. In the other section of the same sample, there is still an outer 40 μm thick microcrystalline SiC layer with some carbon islands underneath but the liquid has penetrated by large channels inside the rod up to its centre. As a consequence, the inner part of the rod is almost completely converted into SiC as shown in Fig. 4. Al_4C_3 has been identified as the main phase forming between the inner and outer SiC. Some small grains of Al_4C_3 have also been observed deep inside the rod. Inside the channels, some well faceted SiC crystals as well as Si crystals formed upon cooling are found.

After 48 hours of treatment, both cross sections of the sample exhibit the same morphology (Fig. 5a). The

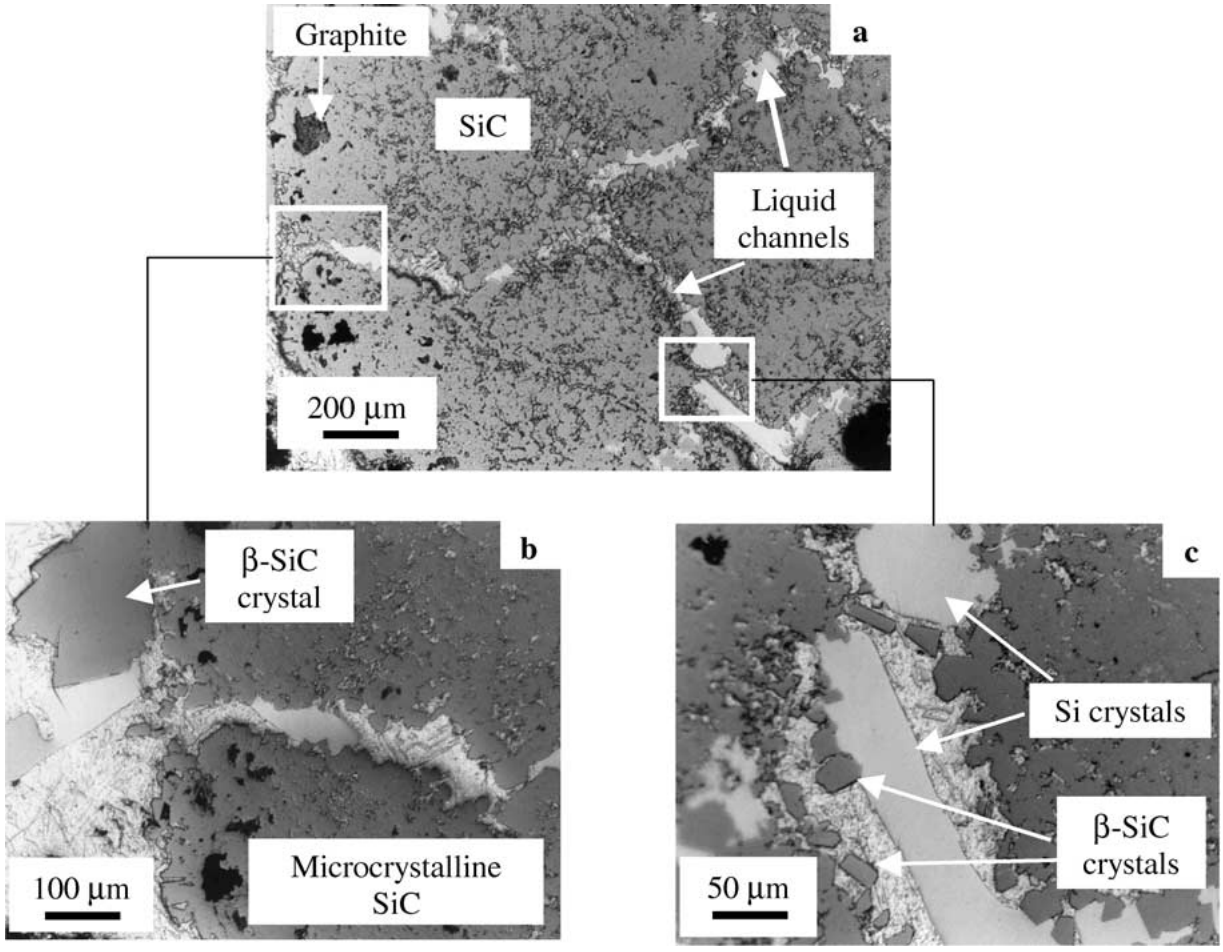

Figure 5 (a) Optical microphotograph showing the cross section of a sample treated at 1100°C for 48 hours with a AS_{30} melt; (b) Close up of the same sample showing a main liquid channel running inside the carbon rod, (c) other close up of the same sample showing the opening of a channel.

graphite rod has been almost completely converted into microcrystalline SiC. Al_4C_3 is no more observed at the periphery of the rod, between inner and outer SiC, and only a few residual graphite grains can be found in that place. Large channels of liquid are running throughout the rod, from the outside to the centre. From these main channels, several small secondary liquid veins are branching off. Al_4C_3 has been identified at the end of these secondary veins. As to the biggest SiC crystals, they are found in or close to the main channels of liquid, either inside the rod or outside (Fig. 5b and c). It has to be noted that large silicon crystals formed on cooling are observable in the free liquid and inside the main channels whereas such crystals cannot be found inside the secondary veins or among SiC microcrystals. This indicates that the Si content of the liquid is higher inside the main channels (about the same composition as that of the free liquid) than in the secondary veins.

3.2. From AS_{20} to AS_{40} experiments

The cross sections of an AS_{25} sample after 14 hours heating (not shown) have appeared similar to the one shown in Fig. 4 and corresponding to an AS_{30} sample after a 28 hours treatment. Indeed, the rod was almost completely converted into SiC. Al_4C_3 was present at the periphery of the rod with unreacted graphite. However, with regard to Fig. 4, the AS_{25} sample showed slight differences such as a more scattered and cracked outer SiC layer and wider liquid channels inside the rod. Moreover, the liquid was more abundant between the SiC microcrystals formed by conversion of the main body of the rod. Finally, the well-shaped SiC crystals were smaller than for an AS_{30} sample.

For an AS_{20} sample annealed during 14 hours, the change in morphology was much more spectacular. As shown in Fig. 6, the rod has no more a cylinder shape. Instead, several aggregates of microcrystalline SiC are randomly scattered in the liquid. There is no more residual graphite and small Al_4C_3 crystals have only been evidenced among the SiC aggregates. In that case, no well-shaped SiC crystals are found.

When the Si content of the melt is increased to 40 at.%, there is much more residual carbon than for an AS_{30} sample after the same reaction time, as can be seen by comparing Figs 7 and 5. Remaining graphite fragments are randomly distributed inside the whole rod and not only at its periphery. The main liquid channels are edged by a dense layer of SiC microcrystals. The outer SiC layer is also denser than usual with almost no liquid inside. Al_4C_3 is present in large amounts in the vicinity of remaining graphite. Between that carbide and the liquid, a thin SiC layer apparently dense is always present.

4. Discussion

We will first discuss the results obtained with AS_{30} samples annealed at 1100°C for various times. In a first stage (up to 15–20 hours heating), the reaction between

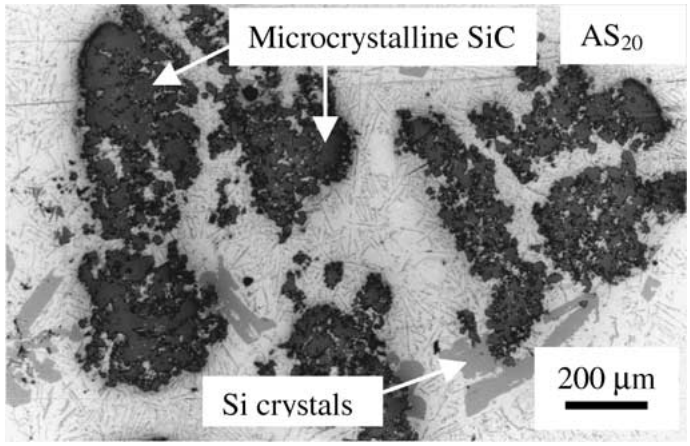

Figure 6 Optical microphotograph showing the cross section of a sample treated at 1100°C for 14 hours with an AS_{20} melt.

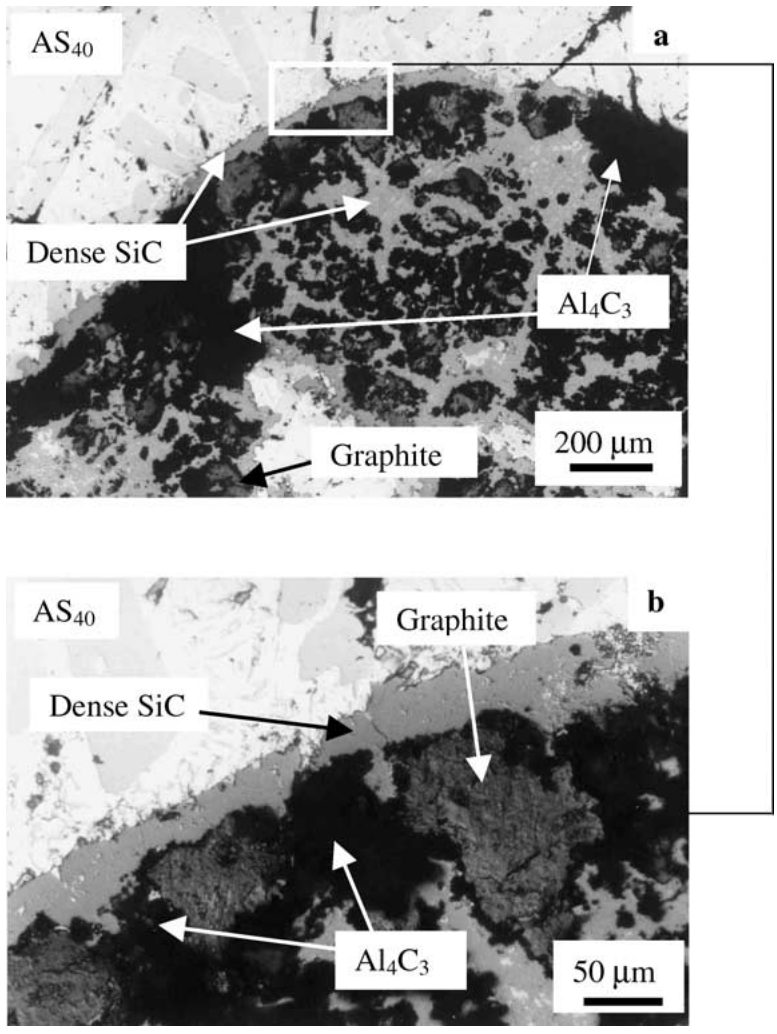

Figure 7 (a) Optical microphotograph showing the cross section of a sample treated at 1100°C for 48 hours with an AS_{40} melt, (b) close up at the periphery of the rod.

the liquid and the graphite rod progresses at a slow rate, a thin and uniform layer of microcrystalline SiC being formed around the rod. The increase in thickness of this outer SiC layer as a function of reaction time is presented in Fig. 8. Because a progressive wetting of the rod surface by the liquid is very likely, we have reported in this graph only the highest values of reaction zone thickness corresponding to the earliest contact at the liquid/graphite interface. By this mean, the time error due to delayed wetting is reduced. It can be seen that in the first stage of interaction, the SiC layer thickness increases quasi-parabolically with the reaction time. As some liquid is often found inside the outer SiC layer (Fig. 3b), the growth mechanism observed here cannot be of a classical solid state diffusion type. Growth should rather proceed by a dissolution-precipitation process. However, as the decrease in growth rate with time is significant, it can be concluded that the SiC

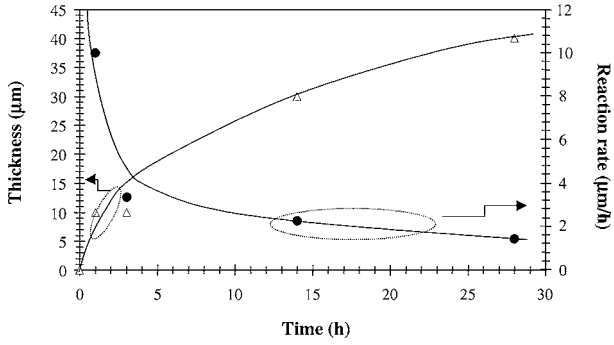

Figure 8 Effect of reaction time on the thickness of the outer SiC layer (△) and on the rate at which graphite is attacked (●).

layer with liquid infiltrated within its constituting microcrystals acts as a semi-permeable barrier. Similar trends have been recently observed for the reaction between liquid silicon and graphite [11].

If the only factor controlling the reaction rate was the liquid infiltration through SiC, the inner part of the rod should not be converted into SiC after 48 hours. Indeed, by extrapolating the curves in Fig. 8, only 50 μm of SiC should be formed after 48 hours whereas a quasi-complete conversion of the rod is observed. Another parameter has then to be taken into account to explain the sudden acceleration of the process of conversion of graphite into SiC involving the rapid penetration of liquid within the rod.

At that point of the discussion, it will be recalled that the liquid has not the same silicon content inside the main channels (about the same content as that of the free liquid) and inside the secondary veins (lower Si content). This is evidenced by the absence of silicon crystals formed upon cooling in the latter whereas such crystals have been observed in the former. Formation of Al_4C_3 at the end of the secondary veins is another indication that the liquid is locally Si poor. Indeed, Al_4C_3 is the stable carbide for low Si content melts [3, 8]. It can be easily understood that consumption of silicon to form SiC in the heart of the rod locally decreases the Si content of the liquid. The Si loss thus created cannot be instantaneously balanced by silicon migration in the narrow veins. Thus a silicon concentration gradient appears in the liquid between the outside and the inside of the rod. The experiments with Si contents in the melt lower than 30 at.% bring some complementary information in the sense that they show that the reaction rate increases when the Si content in the melt decreases. Indeed, it takes only 14 hours to convert all the graphite rod with 20 at.% and 25 at.% Si in the melt whereas only a peripheral SiC layer is formed with 30 at.% Si.

Up to now, we were only considering the simple reactions

$$Si_{(dis)} + C_{(s)} \rightarrow SiC_{(s)} \quad (1)$$

$$4Al_{(dis)} + 3C_{(s)} \rightarrow Al_4C_{3(s)} \quad (2)$$

where $Al_{(dis)}$ and $Si_{(dis)}$ are aluminium and silicon dissolved in the liquid Al-Si alloy. However, these reactions may involve some intermediary steps such as carbon dissolution in the melt and/or silicon, aluminium and carbon liquid diffusion. The solubility of carbon in Al-Si melts is unknown but data are available for the solubility of carbon in pure Al and Si liquids [3, 12]. In pure liquid aluminium, the carbon solubility follows the equation:

$$\log_{10} C_{Al} = 5.5307 - \frac{10335.006}{T} \quad (3)$$

where C_{Al} is the carbon solubility in liquid aluminium expressed in at.% and T the temperature in Kelvin. For the carbon solubility in pure liquid silicon, the following equation can be used

$$\log_{10} C_{Si} = 5.9917 - \frac{14943.603}{T} \quad (4)$$

For example, the solubility of C at 1420°C is 0.26 at.% and 1.46×10^{-3} at.% in pure liquid Al and pure liquid Si, respectively. It would be hazardous to deduce from these equations the carbon solubility in Al-Si melts since some interactions parameters should be taken into account. However, as carbon is much more soluble in aluminium than in silicon it is reasonable to consider that carbon is more soluble in Al rich than Si-rich Al-Si melts. In other words, a decrease in the Si content of the melt should result in an increase of the carbon solubility in the liquid. Consequently, for a low Si content in the melt, the rate of dissolution of carbon should increase. This has indeed been observed with the AS_{25} and AS_{20} samples for which total conversion of the rod into SiC occurred in only 14 hours compared to 28 to 48 hours with 30 at.% Si. Furthermore, with an AS_{20} melt, the reaction was so violent that the rod did not keep its cylinder shape.

Taking into account all these factors, we can propose a reaction mechanism which is summarised in Fig. 9. In places where the liquid wets the rod, a thin SiC layer forms quasi-instantaneously. This layer is microcrystalline with more or less liquid infiltrated within the SiC grains: the higher the Si content of the melt, the denser the SiC layer. As reaction proceeds, the SiC layer thickens and begins to act as a barrier against the penetration of the liquid and the diffusion of silicon in the liquid as shown in Fig. 8. This creates a Si concentration gradient from the outer part (Si rich) to the inner part (Si poor) of the layer. So, the liquid in direct contact with graphite, locally poorer in Si than the free liquid, can dissolve more carbon. Some Al_4C_3 crystals can also form at the C/SiC interface. The presence of Al_4C_3 in almost all the samples is somehow surprising as only SiC is thermodynamically favoured at 1100°C and for Si contents higher than 15% [5]. However, it has been shown that Al_4C_3 could form as a transitory species under non-equilibrium conditions [13].

In some specific sites, the Si content of the liquid is so low that the dissolution rate of carbon becomes very high. Thus, reaction changes from an uniform and smooth attack to a pitting attack, as illustrated by the small dip shown in Fig. 3b. Dissolution locally accelerates and the dip widens to form a crater. The dissolved carbon diffuses towards the outside of the rod where it precipitates into β-SiC crystals as the silicon content

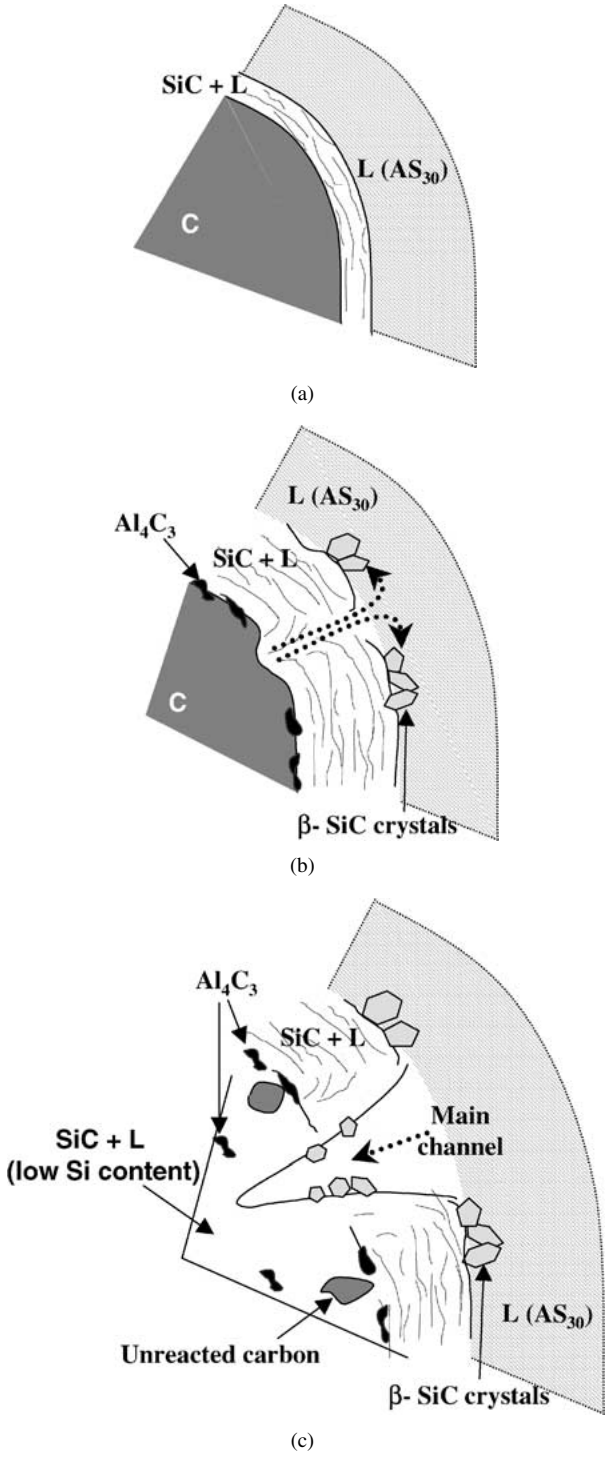

Figure 9 Mechanism of interaction between the carbon rod and the AS_{30} melt: (a) Formation of the outer SiC layer by direct reaction with the liquid; (b) Beginning of the pitting attack by local dissolution of the graphite; (c) total conversion of the rod via the formation of wide channels of liquid.

of the liquid increases. These crystals appear not only near the channel opening (Fig. 5c) but also along the channel walls (Fig. 5b). Note that we could not isolate in our cross sections a more pronounced dip or a wider crater than the one shown in Fig. 3b as these features should be transitory.

It has to be noted that formation of Al_4C_3 or SiC from graphite leads to a relative volume increase $\Delta V/V$ of $+206\%$ and $+137\%$, respectively. In a pitting attack regime, these volume changes can generate enough mechanical stresses to crack the rod and thus to facilitate penetration of the melt. Very likely, it is such a cracking process combined with a very fast reaction rate that explains why the AS_{20} sample shows a so scattered aspect with no memory of the initial cylindrical rod. On the other hand, for AS_{30} or AS_{40} melts, reaction proceeds at a slower rate, cracking is not so important and the initial shape of the rod is retained. In that case, observation of unreacted carbon only under the peripheral SiC layer and not inside the rod suggests that, once liquid channels have attained the centre of the rod, the reaction front progresses from the inside to the outside.

5. Towards LPE experiments

This study has shown that the mechanism of isothermal reaction of an Al-Si melt with a graphite rod depends on the Si content of the liquid. Low Si contents (<25 at.%) increase the reaction rate by favouring the dissolution of carbon and the formation of a porous SiC outer layer. On the other hand, in the presence of a high Si content (>40 at.%), less carbon is dissolved and a dense SiC outer layer is formed. In this study, facetted β-SiC crystals have been only observed near the opening of the main liquid channels at the rod surface or along the walls of the channels inside the rod. These β-SiC crystals have grown in places where a flux of dissolved carbon issuing from the centre of the rod (low Si content) has met a flux of "fresh" silicon migrating in the opposite direction, i.e., from the outside of the rod towards its centre. Because of the increase of its Si content, the liquid in these places has become supersaturated in carbon and favourable conditions for the growth of faceted SiC crystals have been met, whereas in the case of a direct reaction of the liquid with graphite, only SiC microcrystals have formed.

By comparing with a standard LPE process, the isothermal growth of SiC shown here occurs with the same general mechanism: (i) dissolution of carbon in the melt, (ii) carbon transport in the liquid and (iii) SiC growth from a liquid supersaturated in carbon. The main difference between our study and LPE experiments is the way in which carbon supersaturation is achieved. In LPE, a thermal gradient is used whereas in isothermal conditions, a Si concentration gradient is necessary. The former process seems of course easier to achieve and to control experimentally than the latter.

6. Conclusion

We studied the mechanism of reaction between Al-Si melts and calibrated graphite rods in order to elucidate the processes involved in the source zone of LPE experiments. It is shown that reaction proceeds in two steps. First, the liquid reacts at a relatively slow rate to form a continuous microcrystalline SiC layer. When this SiC layer has reached a certain thickness, a violent attack follows on some specific sites by rapid dissolution of the rod along liquid channels extending up to its centre. From that time, the reaction front moves outwards from the heart of the rod to its periphery. The key parameter for that change in the reaction mechanism is the local Si content of the melt which determines the carbon solubility. Some well-shaped β-SiC crystals are observed

to grow from the liquid in places where the dissolved carbon supersaturates because of a locally higher Si content. In LPE experiments, the difficulty will be to achieve and control that carbon supersaturation via a silicon gradient in the liquid.

References

1. R. YAKIMOVA, M. SYVÄJÄRVI and E. JANZÉN, *Mater. Sci. Forum* **264–268** (1998) 159.
2. B. M. EPELBAUM, D. HOFMANN, U. HECHT and A. WINNACKER, *ibid*. **353–356** (2001) 307.
3. L. L. ODEN and R. A. McCUNE, *Metallurgical Transactions* **18A** (1987) 200.
4. S. RENDAKOVA, V. IVANTSOV and V. DMITRIEV, *Mater. Sci. Forum* **264–268** (1998) 163.
5. J. PELLEG, D. ASHKENAZI and M. GANOR, *Mater. Sci. Eng.* A **281** (2000) 239.
6. G. C. YUAN, Z. J. LI, Y. X. LOU and X. M. ZHANG, *ibid*. **280** (2000) 108.
7. F. CHEVRIER, Comptes Rendus Hebdomadaires des Séances de l'Académie des Sciences, Serie C (Sciences Chimiques) **283**(16) (1976) 707.
8. J. C. VIALA, P. FORTIER and J. BOUIX, *J. Mater. Sci.* **25** (1990) 1842.
9. D. CHAUSSENDE, C. JACQUIER, G. FERRO, J. C. VIALA and Y. MONTEIL, *Materials Science Forum* **353–356** (2001) 85.
10. K. LANDRY, S. KALOGEROPOULOU and N. EUSTATHOPOULOS, *Mat. Sci. Eng.* A **254** (1998) 99.
11. A. FAVRE, Thesis, Université de Savoie, France, 1999.
12. C. J. SIMENSEN, *Metallurgical Transactions* **20A** (1989) 191.
13. F. BARBEAU, M. PERONNET, F. BOSSELET and J. C. VIALA, *J. Mater. Sci. Letters* **19** (2000) 2039.

Received 18 April 2001
and accepted 27 March 2002